11th International Workshop on Ship and Marine Hydrodynamics
Hamburg, Germany, September 22-25, 2019

Application of Precise Integration Method for structure dynamics in hydroelasticity computation

Zhe Sun[1]*, Li Zou[1,2,3]

[1]School of Naval Architecture, Dalian University of Technology, Dalian, 116024, P. R. China
[2]State Key Laboratory of Structural Analysis for Industrial Equipment, Dalian University of Technology, Dalian, 116024, P. R. China
[3]Collaborative Innovation Center for Advanced Ship and Deep-Sea Exploration, Shanghai, 200240, P. R. China

*Corresponding author, zsun@dlut.edu.cn

ABSTRACT

In the previous works, the authors have developed a mixed MPS (Moving Particle Semi-implicit) method -- modal superposition model for the highly non-linear hydroelasticity computation [1]. For the structure dynamic part, the rigid and flexible modes are coupled and their mutual effects are considered. The resultant governing equations for the structure part are highly non-linear. In order to further improve the time integration accuracy, the governing equations were first reformulated into ordinary differential equation systems, then the Precise Integration Method (PIM)[2, 3] was used to solve these equations. The dynamics of flexible wedge was simulated by the developed numerical scheme, which showed a better accuracy for long time simulation compared with normal schemes such as Newmark method.

1 INTRODUCTION

The hydroelasticity effect is getting more important due to the increasing of the scales of the modern ships and marine structures [4, 5]. The spring and slamming-induced whipping effects are posing more severe threats for the structure integrity. One of the common features of these highly non-linear fluid and structure interaction phenomena is the transient nature of the dynamics and the large rigid-body motion with relatively small elastic deformation. These characteristics would usually require the time-domain CFD based[6] computation to fully capture the dynamics of the flow. For the structure part, since the deformation is normally elastic, the modal superposition approach is enough to represent the deformation part, however the large rigid-body motion means the mutual effect between rigid-body and flexible parts may affect the overall dynamics of the structural response. Therefore the author has developed a numerical model, which couple particle method based CFD solver (i.e. Modified Moving Particle Semi-implicit Method) and modal superposition method with mutual effect between rigid-body and flexible modes considered, to compute the highly non-linear time domain hydroelasticity problem[1, 7].

For the structural dynamics part, the governing equations usually can be formulated as a set of differential equation systems. For solving the ordinary differential equation systems, Zhong[2, 8] has invented the so-called Precise Integration Method (PIM) , which can provide the accuracy approaching computer hardware precision[2]. Many following improvements have been made to extend the applicability to various non-linear system or large scale problems[3]. In this paper, the PIM is first applied for solving the structural dynamics part in hydroelasticity computations.

The remaining part of the paper is organized as follows: the structural solver based on modal superposition and the implementation process of PIM for such problems are illustrated in Section 2; in Section 3 the results of applying PIM to the 2D flexible wedge dropping in vertical direction are discussed and compared with Newmark Method; the conclusion is drawn in Section 4.

2 METHODOLOGY

In this section, the methods used in the computation are described, i.e. the governing equations for the structural dynamics in hydroelasticity modelling and the implementation process of PIM.

2.1 Structure solver based on modal superposition

As an example of applying PIM for the structural dynamics involved in highly non-linear hydroelasticity problems, the governing equations for the dynamics of a flexible wedge in free fall conditions are given. Since the main focus of this paper is about PIM, only the final governing equations are provided without any derivation, and more details can be found in ref[1].

For a 2D symmetric wedge with flexible bottom as shown in Fig.1, two sets of coordinate systems are established to describe the configuration, i.e. the global fixed *X*-*O*-*Y* system (with the *O*-*X* axis on the undisturbed free surface) and local body-attached s_A-o_A-w_A/s_B-o_B-w_B system. The motion of the wedge is constrained in the vertical direction, as a result its kinetics can be fully described by the position of the tip point Y_R and the deformation of the flexible bottom η_A (or η_B as the configuration and deformation is the same).

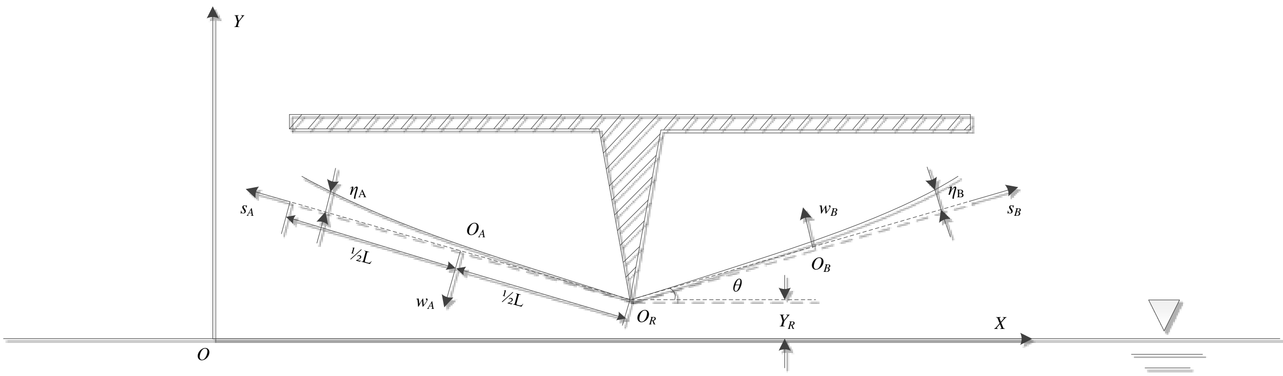

Figure 1: Sketch of the flexible wedge free dropping problem

The elastic deformation is modeled by the modal superposition approach as in Eqn. (1).

$$\eta(s,t) = \boldsymbol{\varphi}^T(s)\mathbf{q}(t) \tag{1}$$

where $\boldsymbol{\varphi}$ and $\mathbf{q}$ are the modal functions and the corresponding generalized coordinates, and their definitions are given in Eqn. (2) and (3).

$$\boldsymbol{\varphi}(s) = \left[\varphi_1(s), \varphi_2(s), \varphi_3(s), ...\right]^T \tag{2}$$

$$\mathbf{q}(t) = \left[q_1(t), q_2(t), q_3(t), ...\right]^T \tag{3}$$

The flexible bottoms are modelled as Euler-Bernoulli beams. The mode functions of these beams are found based on the orthogonal relations, and for a cantilever beam used in this study, the corresponding mode functions are given in Eqn. (4)

$$\varphi_i(s) = \frac{1}{\sqrt{M_b}}\left[\cosh(\frac{2\mu_i s}{L}) - \cos(\frac{2\mu_i s}{L}) - \sigma_i(\sinh(\frac{2\mu_i s}{L}) - \sin(\frac{2\mu_i s}{L}))\right], i = 1,2,3,... \tag{4}$$

where M_b is the mass of each beam, $\sigma_i = \dfrac{\sin(2\mu_i) - \sinh(2\mu_i)}{\cos(2\mu_i) - \cosh(2\mu_i)}$, μ_i is the i^{th} root of the relation $\cos(2\mu_i) + \cosh(2\mu_i) = -1$, and for the first three modes, the values are $\mu_1 = 0.9375, \mu_2 = 2.3470$, $\mu_3 = 3.9274$.

By using the Lagrangian equation, the final governing equations for the dynamics of flexible wedge is derived as follow:

$$
\begin{aligned}
&M_m \ddot{Y}_R + 2\cos(\theta)(\psi_{01}\ddot{q}_1 + \psi_{02}\ddot{q}_2 + \psi_{03}\ddot{q}_3) = Q_{Y_R} \\
&\ddot{Y}_R \cos(\theta)\psi_{01} + \ddot{q}_1 + \omega_1^2 q_1 = Q_{q_1} \\
&\ddot{Y}_R \cos(\theta)\psi_{02} + \ddot{q}_2 + \omega_2^2 q_2 = Q_{q_2} \\
&\ddot{Y}_R \cos(\theta)\psi_{03} + \ddot{q}_3 + \omega_3^2 q_3 = Q_{q_3}
\end{aligned} \tag{5}
$$

where M_m is the total mass of the wedge, ω_i is the i^{th} natural frequency of the beam, and Q_{Y_R} , Q_{q_i} , ψ_{0i} are defined as follows:

$$Q_{Y_R} = \int_{A \ and \ B} p n_y dl - M_m g \tag{6}$$

$$Q_{q_i} = \int_{A \ or \ B} p \varphi_i dl \qquad i = 1,2,3 \tag{7}$$

$$[\psi_{01}, \psi_{02}, \psi_{03}, ...]^T = \int_{-L/2}^{L/2} \boldsymbol{\varphi} \rho_l ds \tag{8}$$

where ρ_l is the line density, g is the acceleration due to gravity, p is the pressure along the wedge bottom.

2.2 Precise Integration Method

2.2.1 Reformulation of the governing equations

In order to use the Precise Integration Method, the governing equation of the dynamic system i.e. Eqn. (5) is first reformulated as Eqn. (9):

$$\mathbf{M\ddot{x} + G\dot{x} + Kx = r} \tag{9}$$

where $\mathbf{x}$, $\mathbf{r}$, $\mathbf{M}$, $\mathbf{G}$ and $\mathbf{K}$ are defined in Eqn. (10)-(14)

$$\mathbf{x} = [Y_R, q_1, q_2, q_3]^T \tag{10}$$

$$\mathbf{r} = [Q_{Y_R}, Q_{q_1}, Q_{q_2}, Q_{q_3}]^T \tag{11}$$

$$\mathbf{M} = \begin{bmatrix} M_m & 2\cos(\theta)\psi_{01} & 2\cos(\theta)\psi_{02} & 2\cos(\theta)\psi_{03} \\ \cos(\theta)\psi_{01} & 1 & 0 & 0 \\ \cos(\theta)\psi_{02} & 0 & 1 & 0 \\ \cos(\theta)\psi_{03} & 0 & 0 & 1 \end{bmatrix} \tag{12}$$

$$\mathbf{K} = \begin{bmatrix} 0 & 0 & 0 & 0 \\ 0 & \omega_1^2 & 0 & 0 \\ 0 & 0 & \omega_2^2 & 0 \\ 0 & 0 & 0 & \omega_3^2 \end{bmatrix} \tag{13}$$

$$\mathbf{G} = [\mathbf{0}] \tag{14}$$

By introducing the new phase space variable $\mathbf{v} = \{\mathbf{x}, \mathbf{p}\}^T$, in which $\mathbf{p}$ is defined in Eqn. (15) , Eqn. (9) can be further reformulated as Eqn. (16)

$$\mathbf{p} = \mathbf{M\dot{x}} + \frac{1}{2}\mathbf{Gx} \tag{15}$$

$$\mathbf{\dot{v} = Hv + f} \tag{16}$$

where the right hand side $\mathbf{f}$ and system matrix $\mathbf{H}$ are defined in Eqn. (17)-(19):

$$\mathbf{f} = \{\mathbf{0}, \mathbf{r}\}^T \tag{17}$$

$$\mathbf{H} = \begin{bmatrix} \mathbf{A} & \mathbf{D} \\ \mathbf{B} & \mathbf{C} \end{bmatrix} \tag{18}$$

$$\mathbf{A} = -\frac{1}{2}\mathbf{M}^{-1}\mathbf{G}, \quad \mathbf{B} = \frac{1}{4}\mathbf{G}\mathbf{M}^{-1}\mathbf{G} - \mathbf{K}, \quad \mathbf{C} = -\frac{1}{2}\mathbf{G}\mathbf{M}^{-1}, \quad \mathbf{D} = \mathbf{M}^{-1} \tag{19}$$

2.2.2 Implementation of PIM[2, 3]

For the system described in Eqn. (16), the solution can be found by using Duhamel integral as in Eqn. (20), in which all the variables in the k^{th} time step $\mathbf{v}_k$ are all assumed to be known.

$$\mathbf{v}_{k+1} = \exp(\mathbf{H}\eta)\mathbf{v}_k + \int_0^\eta \exp\left[(\mathbf{H}(\eta-\tau))\right]\mathbf{f}(t_k+\tau)d\tau \tag{20}$$

The key of the implementing PIM is the way of calculating the value of the matrix exponent $\exp(\mathbf{H}\eta)$. This computation consists of two steps, first the additional theorem of exponential matrix is used to expand the matrix into the form of Eqn. (21).

$$\exp(\mathbf{H}\eta) = \exp(\mathbf{H}\tau)^m, \quad \tau = \eta / m, \quad m = 2^N \tag{21}$$

By properly choosing the value of N (normally 20), the time interval τ could be regarded as a very small value, hence the truncated Taylor expansion can be used to represent Eqn. (21) as in Eqn. (22) and (23):

$$\exp(\mathbf{H}\tau) \approx \mathbf{I} + \mathbf{R} \tag{22}$$

$$\mathbf{R} = \mathbf{H}\tau + (\mathbf{H}\tau)^2/2! + (\mathbf{H}\tau)^3/3! + (\mathbf{H}\tau)^4/4! \tag{23}$$

If we submit Eqn. (22) back to Eqn. (21), matrix exponent can then be approximated as Eqn. (24).

$$\exp(\mathbf{H}\eta) = (\mathbf{I}+\mathbf{R})^{2^N} = \left(\mathbf{I} + 2\mathbf{R} + \mathbf{R}^2\right)^{2^{N-1}} \tag{24}$$

Instead of directly continuing the squaring operation, the formulation in Eqn. (25) is used to update the incremental part, which can avoid the corruption of the accuracy since **I** is a much bigger value than the incremental value of $\mathbf{R}_{(n)}$.

$$\mathbf{R}_{(n)} = 2\mathbf{R}_{(n-1)} + \mathbf{R}_{(n-1)}^2 \tag{25}$$

After repeating N times of this operations, the matrix exponent $\exp(\mathbf{H}\eta)$ can finally be calculated as Eqn. (26)

$$\exp(\mathbf{H}\eta) = \mathbf{I} + \mathbf{R}_{(N)} \tag{26}$$

For the integral part of Eqn.(20), the Gauss Integration Quadrature can be used as in Eqn. (27).

$$\int_0^\eta \exp\left[\mathbf{H}(\eta-\tau)\right]\mathbf{f}(t_k+\tau)d\tau = \frac{\eta}{2}\sum_{i=1}^{k} w_i \exp\left[\mathbf{H}\left(\eta - (1+\tau_i)\eta/2\right)\right]\mathbf{f}(t_k + (1+\tau_i)\eta/2) + O(\eta^{2k}) \tag{27}$$

in which the matrix exponent $\exp\left[\mathbf{H}\left(\eta-(1+\tau_i)\eta/2\right)\right]$ is calculate in the same way as Eqn. (21)

3 RESULTS AND DISCUSSIONS

In this section, the performance of the PIM is briefly analysed by comparing with the widely used Newmark Method (NM)[9] for a system as Eqn. (9). No artificial damping is used in the NM integration model. A unit constant force is applied to the tip of the wedge pointing to the *O-Y* direction, which means $Q_{Y_R} = 1$ and $Q_{q_i} = 0, \; i = 1,2,3$. Three different time intervals are used to test the integration performance.

The time history of the vertical displacement and the general coordinate q_1 are shown in Fig. 2-5. As shown in Fig. 2 and 3, the vertical displacement Y_R calculated by NM and PIM are very similar. They are not sensitive to the time steps, and both of them are capable of providing quite accurate result even under large time interval such as 1s.

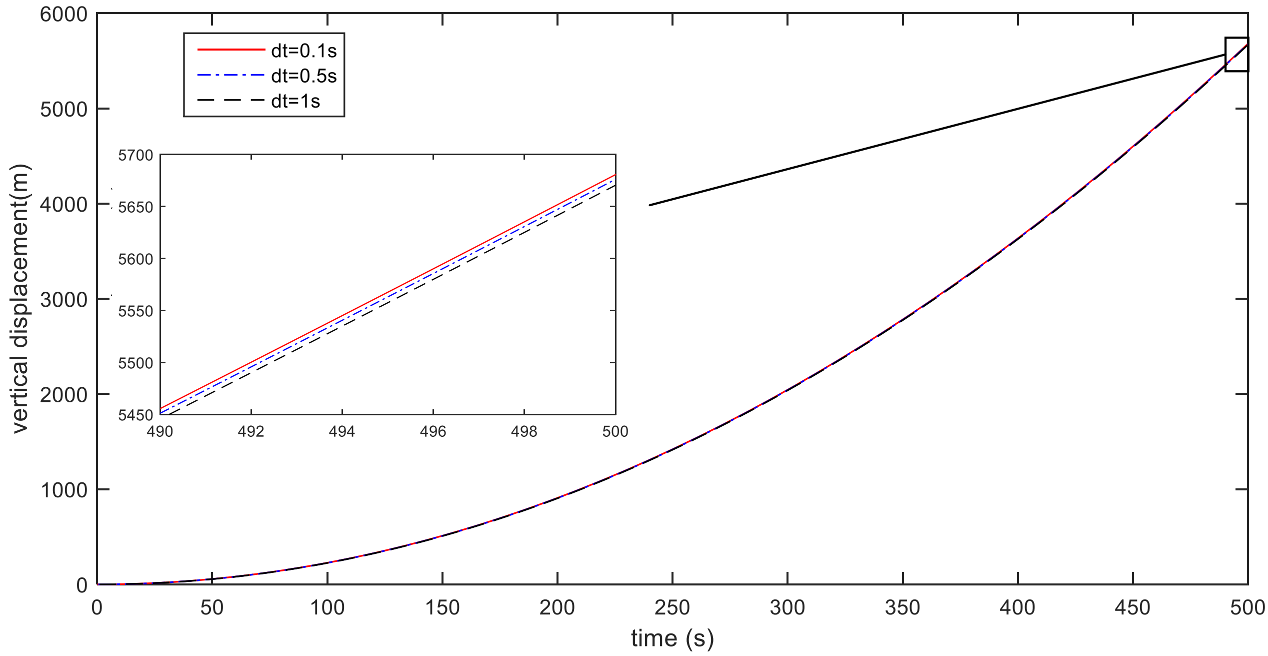

Figure 2: *Y* displacement by PIM.

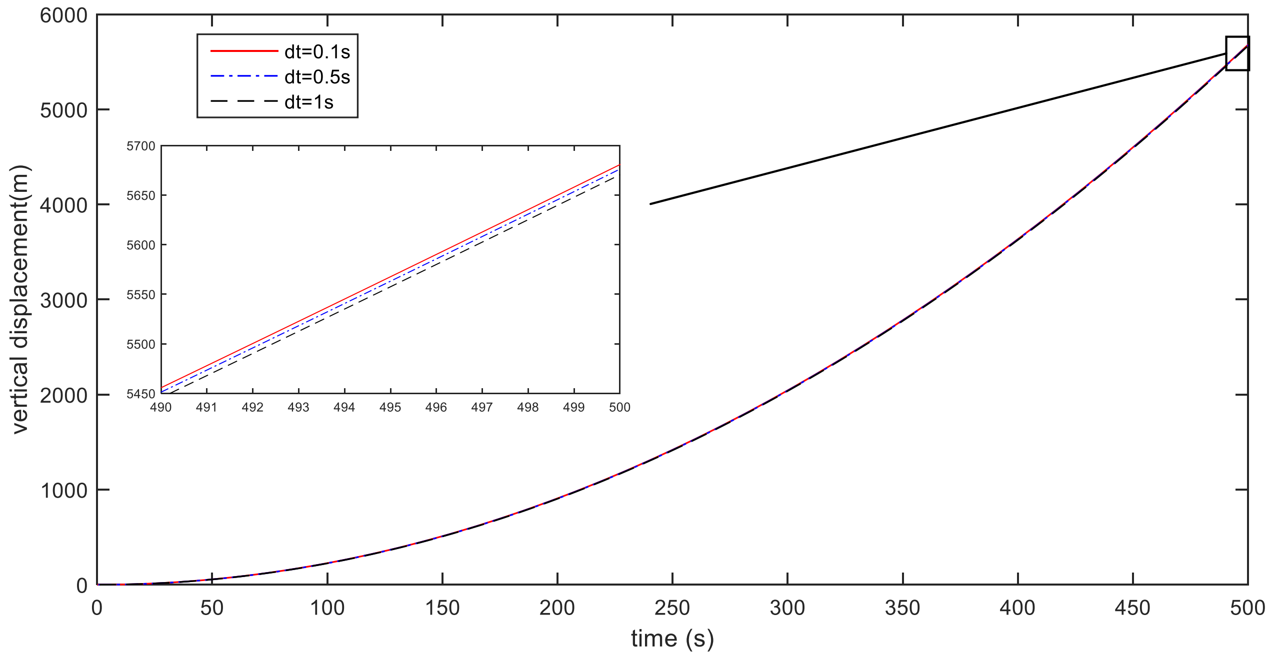

Figure 3: *Y* displacement by NM.

For the deformation part, as shown in Fig. 4 and 5, the maganitude of the oscillations are almost the same by using either NM or PIM. However, the phase shiftting can be very severe under large time steps such as 1s in NM (Fig. 5). This indicates that the Precise Integration Method has very good stability and high accuracy even under extreme computational conditions. In terms of computation time, the single time step for NM and PI would take 0.004s and 0.005s respectively. This is caused by the slightly complicated martix manipulations in PI than NM. But considering that the time step in PI could be significantly larger than NM for similar accuracy, the overall effeciency of PI is still higher than NM.

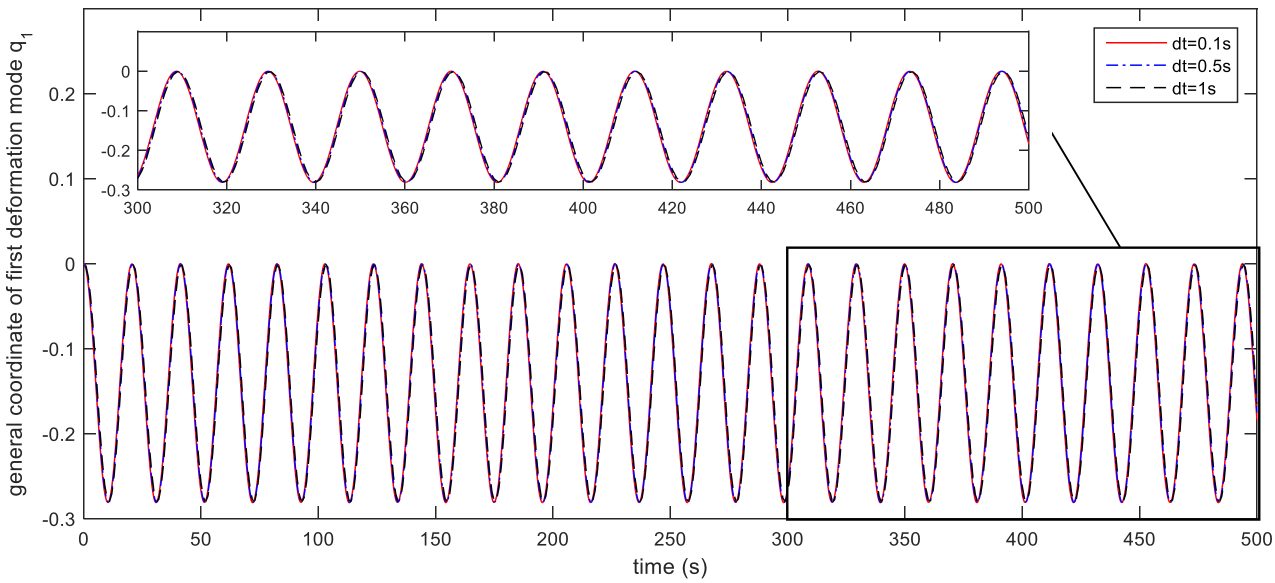

Figure 4: General coordinate q_1 by PIM.

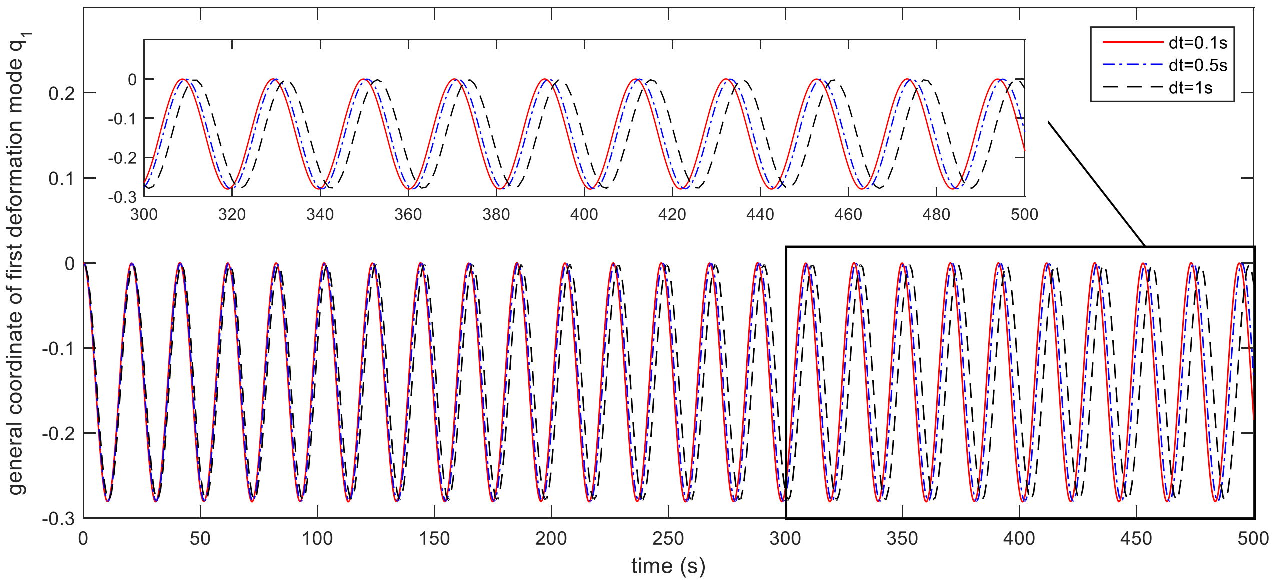

Figure 5: General coordinate q_1 by NM

4 CONCLUSION

In this paper, the Precise Integration Method is used to further improve the integration accuracy of the structural model of hydroelasticity computation. The governing equations for the coupled rigid-body and elastic deformation modes model for a 2D symmetric wedge dropping case is first provided, then the implementation details of the PIM for this model is formulated. The preliminary results show that the PIM can give more accurate and stable results for very large time steps, compared with the well-known Newmark method. The performance of this approach for more complex structural model is planned to be investigated in the future study.

ACKNOWLEDGEMENTS

This work is supported by the National Natural Science Foundation of China (No.51809035), Fundamental Research Funds for the Central Universities (DUT19RC(4)028, DUT2017TB05), to which the authors are most grateful.

REFERENCES

[1]. Sun, Z., et al., "Modified MPS method for the 2D fluid structure interaction problem with free surface". In: *Computers & Fluids*. 122(2015), 47-65.
[2]. Zhong, W.-X., "On precise integration method". In: *Journal of Computational and Applied Mathematics*. 163(2004), 59-78.
[3]. Gao, Q., S. Tan, and W. Zhong, "A survey of the precise integration method". In: *SCIENTIA SINICA Technologica*. 46(2016), 1207-1218.
[4]. Malenica, S. and Q. Derbanne, "Hydro-structural issues in the design of ultra large container ships". In: *International Journal of Naval Architecture and Ocean Engineering*. 6(2014), 983-999.
[5]. Temarel, P., et al., "Prediction of wave-induced loads on ships: Progress and challenges". In: *Ocean Engineering*. 119(2016), 274-308.
[6]. Seng, S., J.J. Jensen, and Š. Malenica, "Global hydroelastic model for springing and whipping based on a free-surface CFD code (OpenFOAM)". In: *International Journal of Naval Architecture and Ocean Engineering*. 6(2014), 1024-1040.
[7]. Sun, Z., et al., "Numerical analysis of violent hydroelastic problems based on a mixed MPS-mode superposition method". In: *Ocean Engineering*. 179(2019), 285-297.
[8]. Zhong, W.-X. and Z.-s. Yang, "On the computation of the Main Eigen-Pairs of the Continuous-Time Linear Quadratic Control Problem". In: *Applied Mathematics and Mechanics*. 12(1991).
[9]. Newmark, N.M., "A Method of Computation for Structural Dynamics". In: *Journal of the Engineering Mechanics Division*. 85(1959), 67-94.